Motion of actin filaments in the presence of myosin heads and ATP

S. Burlacu and J. Borejdo
Baylor Research Institute, Baylor University Medical Center, Dallas, Texas 75226 USA

ABSTRACT We measured, by fluorescence correlation spectroscopy, the motion of actin filaments in solution during hydrolysis of ATP by acto-heavy meromyosin (acto-HMM). The method relies on the fact that the intensity of fluorescence fluctuates as fluorescently labeled actin filaments enter and leave a small sample volume. The rapidity of these number fluctuations is characterized by the autocorrelation function, which decays to 0 in time that is related to the average velocity of translation of filaments. The time of decay of the autocorrelation function of bare actin filaments in solution was 10.59 ± 0.85 s. Strongly bound (rigor) heads slowed down the diffusion. Direct observation of filaments under an optical microscope showed that addition of HMM did not change the average length or flexibility of actin filaments, suggesting that the decrease in diffusion was not due to a HMM-induced change in the shape of filaments. Rather, slowing down of translational motion was caused by an increase in the volume of the diffusing complex. Surprisingly, the addition of ATP to acto-HMM accelerated the motion of actin filaments. The acceleration was the greatest at the low molar ratios of HMM:actin. Direct observation of filaments under an optical microscope showed that in the presence of ATP the average length of filaments did not change and that the filaments became stiffer, suggesting that acceleration of diffusion was not due to an ATP-induced increase in flexibility of filaments. These results show that some of the energy of splitting of ATP is imparted to actin filaments and suggest that 0.06 ± 0.02 of HMM interferes with the diffusion of actin filaments during hydrolysis of ATP.

INTRODUCTION

In the "classical" hypothesis of muscle contraction, the myosin head hydrolyses ATP while it is dissociated from actin (Lymn and Taylor, 1971). Heads carrying the products of hydrolysis bind to filaments either "weakly" or "strongly." Only strongly bound heads continue along the ATPase cycle whereby the products of hydrolysis are released (Podolsky, 1980; Goldman et al., 1984). The release is believed to be associated with the orientational change of S1 (Huxley, 1969) and is followed by dissociation from actin. In solution, the interaction between myosin and actin has no effect on translational motion of myosin heads (Borejdo, 1979; Borejdo and Burlacu, 1992*a*). In this work we test whether the interaction has an effect on translational motion of actin filaments.

Oosawa et al. (1973) measured motion of F-actin during splitting of ATP by HMM using quasi-elastic light scattering (QELS). They saw a decrease in the width of the spectrum of scattered light when ATP was being hydrolyzed and concluded that F-actin became more flexible during hydrolysis. On the other hand, Fraser et al. (1975) reported that the spectrum of quasi-elastically scattered light remained unchanged during maximal activation of HMM ATPase by actin. Tirosh et al. (1990) reported the broadening of spectrum of quasi-elastically scattered light from acto-HMM during hydrolysis. Interpretation of QELS data is complicated by the fact that QELS records the light scattered by both F-actin and HMM and this is particularly troublesome at high protein concentrations. Yanagida et al. (1984) directly observed diluted actin filaments in an optical microscope and concluded that in the presence of HMM and ATP filaments executed more rapid bending motions and were often broken into short segments.

We studied the effect of the cyclic interaction of HMM with actin on the motion of actin filaments by the method of fluorescence correlation spectroscopy (FCS). This avoids complication of QELS associated with light scattering by both proteins. This method relies on the fact that when fluorescently labeled actin filaments diffuse through a small volume they give rise to fluctuations in fluorescent light intensity because the observed number of filaments changes in time as they enter and leave the volume. The rapidity of number fluctuations is characterized by the autocorrelation function (ACF), which decays with a characteristic time related to the translational diffusion coefficient of the diffusing species (Elson and Magde, 1974; Magde et al., 1974). Analysis of fluctuations is a method of choice because fluctuations are large (average number of molecules in sample volume is small), FCS measures motion only of labeled F-actin and the motion of very dilute solutions of F-actin can be detected. The results show that actin filaments having strongly bound heads moved slower than bare actin. Surprisingly, when ATP was added to the HMM-actin complex at low molar ratio, the diffusion of actin filaments was accelerated. The acceleration was not caused by a decrease in the average length or by an increase in the flexibility of filaments. Rather, the increase in the rate of diffusion was due to the fact that some of the energy of hydrolysis of ATP by acto-HMM was imparted to actin filaments. The acceleration was progressively diminished at increasing molar ratio HMM:actin. From the relationship between the characteristic time of diffusion and molar ratio we estimated that 0.06 ± 0.02 of HMM retarded diffusion of filaments in the presence of ATP.

Address correspondence to Dr. Julian Borejdo, Baylor University Medical Center, 3812 Elm Street, Dallas, TX 75226.

MATERIALS AND METHODS

Optics and electronics

The experimental microscope system used to measure the fluctuations in fluorescence intensity caused by the translating actin filaments was the same as described before (Borejdo and Burlacu, 1992*b*), except that the motion occurred in solution (in three dimensions) rather than on the surface of a cover slip (in two dimensions). To observe the motion, the experimental cells were constructed by gluing by a superglue (Adhesive Solutions, Sydney, Australia) two narrow strips of a coverslip to a glass slide. The strips were separated by about 1 cm. The experimental chamber was constructed by gluing a coverslip to the top of the strips. The chamber ($\approx 100\ \mu L$) was filled with the solution to be studied and sealed with a colorless nail polish. The concentration of actin was 50 nM. Sample volume was defined by the laser beam and the field diaphragm. To make sure that the same sample volume was always sampled, the image of the coverslip was obtained first and the objective (Plan ×40, N.A. = 0.65; Carl Zeiss, Oberkochen, Germany) was then lowered by a fixed distance. Thus the objective was always focused on the same plane lying between coverslip and the microscope slide. A circular field diaphragm (diameter in the image plane, $D = 10\ \mu m$) was centered on the intensity maximum of the image of the laser beam.

S/N ratio

The fact that the motion occurs in three dimensions and that the confocal arrangement is used (i.e., the field diaphragm is incorporated) complicates the interpretation of the data. When moving molecules are confined to the plane of focus of the objective (i.e., when movement is two-dimensional), each fluorophore within the acceptance angle of the objective contributes equally to the measured signal (in spite of the fact that the original FCS experiment (Magde et al., 1974) was carried out in solution, the diffusion was really two-dimensional because the incident laser beam was focused by a long focal-length lens). In our earlier work (Borejdo and Burlacu, 1992*b*) the diffusion was truly two-dimensional. Under the conditions used in the present experiment, however, this is no longer true: the fluorophores located farther from the focal plane of the objective contribute less to the total fluorescence intensity (Qian and Elson, 1991). The rate of detection of fluorescent photons per molecule of dye during one bin width, σ, which determines the signal-to-noise ratio (S/N, Magde et al., 1974) is now related to the laser light flux by the collection efficiency function, which is dependent on the diameter of the diaphragm, acceptance angle of the objective, and the intensity profile of the exciting laser beam. Analytical expressions for the collection efficiency function exist (Qian and Elson, 1991), but we did not use them for the purpose of an estimation of S/N. Instead, we estimated σ as if the diffusion occurred in two dimensions. The justification for this is given in a section describing diffusion of microspheres. As shown in Borejdo and Burlacu (1992*b*) in the two-dimensional diffusion of F-actin the parameter σ is

$$\sigma = \langle n \rangle / (400 L_n \langle N \rangle) \qquad (1)$$

where $\langle n \rangle$ is the rate of arrival of photons during one bin width, 400 is the number of rhodamine molecules per 1 μm of actin filament (equal to number of actin monomers/1 μm), L_n is the average length of actin filament and $\langle N \rangle$ is the average number of actin filaments in the experimental volume. $\langle N \rangle$ observed by the photomultiplier is equal to the reciprocal of the mean rms fluctuation, β, (Elson and Magde, 1974)—$\langle N \rangle = 1/\beta$. In the typical experiment (Fig. 5) β was 4.3%. Therefore $\langle N \rangle$ was typically 23. In the same experiment $\langle n \rangle$ was 23,036. L_n = 2.37 (Fig. 10 *A*) and therefore $\sigma = \langle n \rangle / (400 \langle N \rangle L_n) = 1.05$. This is a large number, and is obtainable only because we are observing slow motions of a small number of molecules.

Koppel (1974) and Magde et al. (1974) have shown that when σ is greater than or equal to 1, then

$$S/N = (M \delta\tau / 2\tau_D)^{1/2} \qquad (2)$$

where M is the total number of bins collected, $\delta\tau$ is the bin width, and τ_D is the characteristic time of the autocorrelation function. In a typical experiment, $M = 4096$, $\delta\tau = 200$ ms, and $\tau_D = 7$ s giving $S\ N = 7.6$.

Systematic errors

These could arise because of photobleaching of fluorescence. However, all our solutions contained a deoxygenating system (Englander et al., 1987), the light flux was low (incident intensity was typically 0.15 mW), and a continuous exchange of bleached actin molecules for unbleached ones occurred. The quantum yield for photobleaching, which was measured by following the decrease in emitted light intensity of actin filaments attached to a cover slip was less than 10^{-11}. Lifetime for bleaching was about 500 s, much longer than the characteristic time for translation of actin filaments (see below).

Data analysis

This was done as described previously (Borejdo and Burlacu, 1992*b*), except that the number of "sweeps" was now 6. Also, all sweeps where experimental rms fluctuations exceeded by 30 times the fluctuations of white noise signal having the same $\langle n \rangle$ were rejected in order to eliminate contributions to the signal from dust particles, which sometimes traversed the experimental volume. For example, in the experiment illustrated in Fig. 5 the mean count was 23,063 counts/bin. If this count were contributed by a signal with a white noise characteristic, then fluctuation would have been 151 counts/bin. All sweeps having rms fluctuation of more than 4,530 counts/bin would have been rejected.

Materials

TRITC-phalloidin, ATP, DTT, the enzymes used in the deoxygenating solution and apyrase were from Sigma Chemical Co. (St. Louis, MO). Fluorescent beads (Fluoresbrite) were from Polysciences Inc. (Warrington, PA). Nitrocellulose was from Ernest F. Fullam Inc. (Latham, NY).

Solutions

Diffusion was measured in A-buffer containing 25 mM K-Acetate, 25 mM TRIS-Acetate buffer (pH 7.5), 4 mM Mg_2SO_4, 1 mM DTT, 1 mM EGTA, and oxygen scavenging system (Englander et al., 1987). When indicated, solution also contained 2 mM MgATP. Phalloidin was prepared as follows: 0.1 mg was dissolved in 0.1 ml of 50% methanol and diluted ten times with 25 mM K-Acetate, 25 mM Tris-Acetate (pH 7.5).

Protein preparation and labeling

Actin and HMM were prepared according to Spudich and Watt (1971) and Weeds and Pope (1977), respectively. F-actin was labeled with TRITC-phalloidin by adding 0.05 mg/ml protein to equimolar concentration of the dye and incubating overnight on ice. After staining, F-actin was diluted with A-buffer to 50 nM. Proteins were checked by SDS-PAGE and by the ability to induce motions in vitro motility assay.

Measurements of lengths of actin filaments

The spatial resolution of the optical microscope is 0.19 μm. The images on the video monitor were magnified 2,750 times and any luminous object that was shorter than $\approx$1.1 mm on the monitor screen was counted but its length was not measured. The width of a single filament is smaller than the resolution of the optical microscope and is visible due to the "magnification anisotropy" (Houseal et al., 1989).

The individual frames were grabbed from the VCR using an MV1

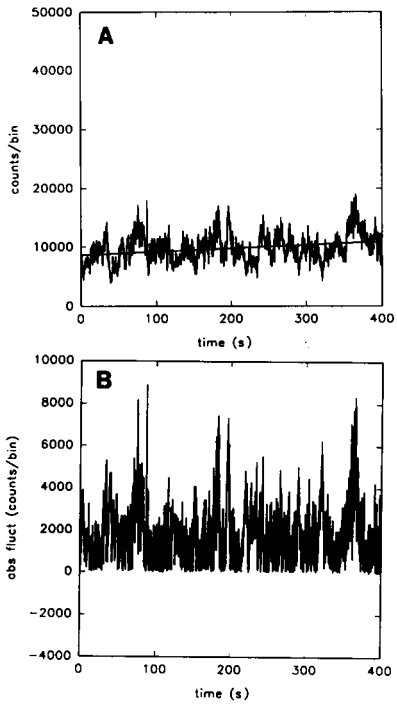

FIGURE 1 Fluctuations in the concentration of 1 μm diameter microspheres (A) photocurrent. The straight line is the linear regression of all data points. The average photocounts value was $\langle n \rangle$ = 9752, SD = 235 (B) absolute fluctuations of the signal in A (the absolute value of the difference between each data point and the corresponding regression value).

frame grabber (MetraByte Corp, Taunton, MA) operated by an AT type computer. The images were contrast enhanced by a video analysis program (Java 1.4; Jandel Scientific, Corte Madera, CA), equalized using Gray F/X gray scale editor (Xerox Imaging Systems, Sunnyvale, CA) and printed on Video Printer (Sony Corp., Teaneck, NJ) or Linotronic 300 typesetter. Contour lengths of filaments were measured by using the "distance" function of Java image analysis program. The histograms were obtained by counting "by range" filaments of a given length. They were plotted using SigmaPlot 4.1 (Jandel Scientific).

RESULTS

Diffusion of microspheres

In a confocal microscope system such as used here, the decay time of the ACF of a three-dimensional diffusion of particles depends on the relative size of the diaphragm and the diameter of the laser beam (Qian and Elson, 1991). For example, when the diaphragm is smaller than the "beamwaist" of the laser, then the diffusion along the line of excitation becomes important, and the shape of the ACF, as derived from two-dimensional analysis, is no longer valid. Detailed analysis of the optics of the measurement system is therefore required in order to obtain exact expression for the ACF (Qian and Elson, 1990). Our experiment is further complicated by the fact that the size of diffusing objects is comparable to the depth of focus of the objective. To find the best way to fit the data obtained under our experimental conditions, we carried out empirical calibrations using particles with well characterized diffusion coefficients. Calibration shows that in our experiments the best fit is offered by two exponents.

We measured the ACF of a monodisperse suspension of particles of size similar to actin filaments. We used fluorescent polystyrene latex microspheres 1 $\pm$ 0.05 μm in diameter diluted with water to about 5–50 $\times$ 10^6 particles/mm^3. Fig. 1 A shows a typical photocurrent signal of spheres. Fluctuations in the photocurrent arise because spheres move by Brownian motion in and out of the field of view defined by the diaphragm. The mean rate of arrival of photons $\langle n \rangle$ was 9,762 counts/bin. The absolute fluctuation (Fig. 1 B) was 2,352 counts/bin (relative fluctuation β = 24%). If the signal had white noise characteristics, the fluctuation would have been $(9762)^{1/2}$ = 99 counts/s (1%; Rabiner and Gold, 1975). In this experiment the observed fluctuation was 24 times greater than the fluctuation expected from the white noise signal. β was large because the number of spheres in the field of view was small.

The average normalized ACF of all nine microsphere experiments is shown in Fig. 2. The rapid decay occurred in about 3 s and was followed by a slow decay. The overall decay was fitted well by a double exponential (see below). All ACFs had a periodic component. We suspect that oscillations were due to the presence of the diaphragm, i.e., to the fact that when particle diffused out of the sample volume the fluorescence decayed rapidly to 0.

The characteristic time of the decay of the correlation, τ_D, is a measure of the rapidity of motion. We have extracted τ_D from the autocorrelation function in four ways: (a) manually—τ_D was defined as the time at which normalized ACF declined to 0.5, (b) by a single exponential fit ACF = $A \exp(-\tau/\tau_D)$; (c) by a double exponential fit ACF = $A \exp(-\tau/\tau_D) + B \exp(-\tau/\tau_X)$; and ($d$) by a hyperbolic fit ACF = $A[1 + \tau/\tau_D]^{-1}$ where

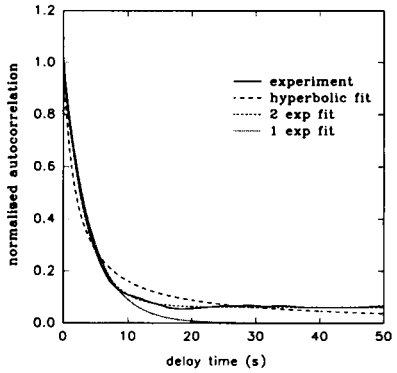

FIGURE 2 Normalized autocorrelation function of 1 μm microspheres (average of 9 experiments): experimental curve (*solid line*), hyperbolic fit (*large dashed line*), double exponential fit (*small dashed line*), single exponential fit (*dotted line*).

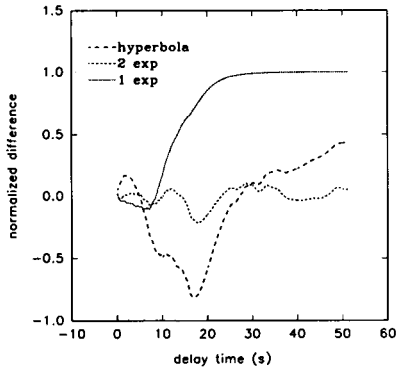

FIGURE 3 The normalized difference between the fitting curves and the experimental autocorrelation function (see text for details). Symbols used are the same as in Fig. 2.

A, B, and τ_X are constants and τ_D is the characteristic time. As a figure of merit for the goodness of fit we used the normalized residual N: N = square root of the sum of squares of residuals of the Marquardt–Levenberg fit. Manual fit to the average of all sphere experiments gave $\tau_D = 2.50$ s. Double exponential fit gave $A > B$, $\tau_D < \tau_X$, $\tau_D = 3.35$ s, $N = 0.12$. Single exponential fit gave $\tau_D = 4.16$ s, $N = 1.18$. Hyperbolic fit gave $\tau_D = 1.92$ s, $N = 0.80$. Fig. 3 is a plot of normalized differences $Y = (y_{fit} - y_{exp})/y_{exp}$ versus the delay time τ for three different fits. Double exponential fit was the best because Y was the smallest and because it did not systematically increase at the long delay times. This was also true for ACFs of actin preparations (see Fig. 7). In what follows, the characteristic time τ_D was always given as a decay of a first exponent in the double exponential fit to ACF. Because the magnitude of the second exponent was small and because τ_X was large, we speculate that the first exponent reflected the diffusion in the plane perpendicular to the direction of propagation of light, and the second exponent diffusion along the direction of propagation of light.

The mean τ_D for all sphere experiments was $\tau_D = 3.18 \pm 0.20$ s (mean ± SEM of nine experiments; it is not exactly equal to the characteristic time of the mean ACF from Fig. 2, because τ of the mean ACF ≠ mean of τ's). Minimum and maximum values were 2.30 and 3.65 s, respectively. The coefficient of variation was 18.9%.

In the two-dimensional case $\tau_D = \omega^2/4D_D$, where D_D is the diffusion coefficient for solute D (Elson and Magde, 1974). Therefore the diffusion coefficient for spheres $D_D = \omega^2/4\tau_D$ is $0.31 \times 10^{-8} \pm 0.02$ cm^{2}s^{-1} (ω = 2 μm). The theoretical value for the diffusion coefficient of spheres 1 μm in diameter at room temperature is 0.42×10^{-8} cm^2 sec^{-1} (Tanford, 1963) in good agreement with observations.

This agreement, together with the fact that in our experiments the radius of the diaphragm (5 μm) was 2.5 times greater than the beamwaist of the laser (2 μm, calculated value) indicates that the two-dimensional analysis of our three-dimensional experiment is valid (Qian and Elson, 1991).

Actin filaments

The appearance of actin filaments in solution as seen by the photomultiplier (through a 10-μm diaphragm) is shown in Fig. 4. The image of the filaments is poor because fluorescent light is arriving from different planes within the experimental volume and because filaments move rapidly by Brownian motion, which caused technical difficulties in transferring the image from the VCR tape to the computer.

Fig. 5 A shows a representative photocurrent signal of actin filaments. As in the case of microspheres, fluctuations in the photocurrent arise because actin filaments, propelled by random temperature fluctuations (Brownian motion), move in and out of the field of view defined by the diaphragm. The mean rate of arrival of photons $\langle n \rangle$ was 23,063 counts/bin. The absolute rms fluctuation (Fig. 5 B) was 998 counts/bin (relative fluctuation $\beta = 4.3\%$). If the signal had white noise characteristics theoretical fluctuation would have been $(23{,}063)^{1/2} = 151$ counts/s (0.66%). In this experiment the observed fluctuation was 6.6 times greater than the fluctuation expected from the white noise signal. β was large because the number of actin filaments in the field of view was small (23).

To average the results, normalized ACFs of all experiments were added and divided by the number of experiments. Average ACF is shown in Fig. 6. As in the case of microspheres, double exponential fit gave the best fit. Fig. 7 is a plot of normalized differences $Y = (y_{fit} -$

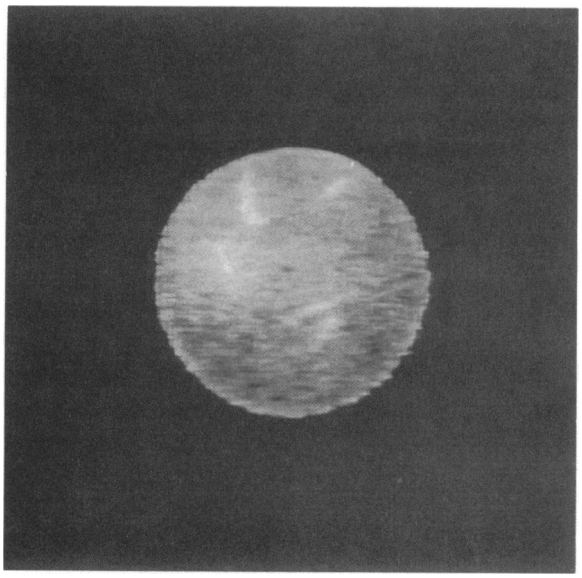

FIGURE 4 Image of actin filaments labeled with TRITC-phalloidin as seen through the 10 μm diaphragm. Filaments free in solution in 25 mM K-acetate, 4 mM Mg-acetate, 1 mM EGTA, 20 mM DTT, 25 mM Tris-acetate (pH 7.5) and an oxygen-removing enzyme complex.

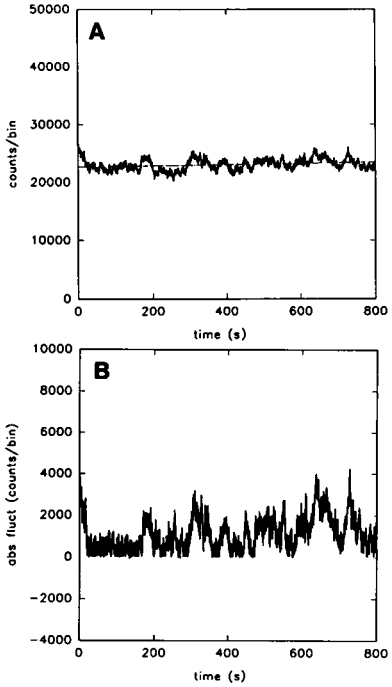

FIGURE 5 (A) Typical photocurrent for a sample of 50 nM actin filaments conplexed with TRITC-phalloidin. The straight line is the linear regression of all data. $\langle n \rangle$ = 23,063 and SD = 998. (B) absolute fluctuations of the signal in A (the absolute value of the difference between each data point and the corresponding regression value).

$y_{exp})/y_{exp}$ versus the delay time τ for 3 different fits. Double exponential fit was the best because Y was the smallest and because it did not systematically increase at the long delay times. N = square root of the sum of squares of residuals of the Marquardt–Levenberg was 0.58, 1.48, 0.17 for hyperbolic, single exponential, and double exponential fit, respectively. For double exponential fit, $A \gg B$, $\tau_D \ll \tau_X$, τ_D = 10.59 s.

The mean τ_D for all actin filaments was $\tau_D = 10.59 \pm 0.85$ s (mean ± SEM of nine experiments; as in the case

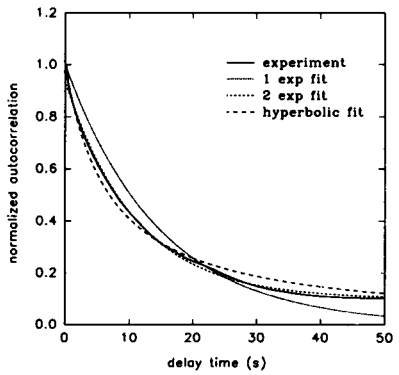

FIGURE 6 Normalized autocorrelation function (average of 9 measurements) of 50 nM TRITC-phalloidin labeled F-actin in A-buffer: solid line, experimental curve; large dashed line, hyperbolic fit; small dashed line, double exponential fit; dotted line, single exponential fit.

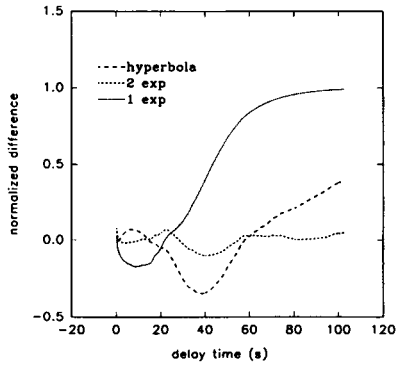

FIGURE 7 The normalized difference of between the fitting curve and the experimental autocorrelation function (see text for details). Symbols used are the same as in Fig. 6.

of microspheres, it is not exactly equal to the characteristic time of the mean ACF from Fig. 6, because τ of the mean does not equal the mean of τ's). Minimum and maximum values were 7.30 and 12.78 s, respectively. The coefficient of variation was 24%.

Two-dimensional analysis of actin data using $D_D = \omega^2/4\tau_D$ gave a diffusion coefficient $0.94 \times 10^{-9} \pm 0.07 \times 10^{-9}$ cm^2 s^{-1} (ω = 2 μm). If we define the average velocity of motion of F-actin, $V_{F\text{-}ACTIN}$, as the ratio of the diameter of the diaphragm (D = 10 μm) to the characteristic time τ_D, then $V_{F\text{-}ACTIN} = D/\tau_D = 0.94 \pm 0.07$ μm/s.

Acto-HMM

When increasing amounts of HMM were added to actin in the absence of ATP, the correlation time progressively increased (diffusion coefficient decreased). This is illustrated in Fig. 8 A, which shows representative correlation functions of actin alone (dotted line), acto-HMM complex at MR of HMM:actin of 1:8 (line b) and the complex at a MR of HMM:actin of 1:2 (line c). Data from all the experiments is summarized in Fig. 8 B. Here the characteristic time of the rigor complex is plotted versus the molar ratio HMM:actin. For comparison, the range of characteristic times of actin filaments alone is shown (all characteristic times of actin filaments ± SEM are contained in the shadowed area). The characteristic time increased from the minimum of 11.43 ± 2.33 s at the MR of HMM:actin = 0.25 to the maximum of 18.51 at the ratio HMM:actin of 4 (the velocity decreased from a maximum of $V_{ACTO\text{-}HMM} = 0.88 \pm 0.17$ μm/s to $V_{ACTO\text{-}HMM} = 0.54$ μm/s.

The most likely reason for the increase in the characteristic time with addition of HMM was an increase in the volume of the complex. However, the characteristic time could also increase if HMM increased the average length or stiffness of actin filaments. To test the effect of HMM on the length, we made direct observations of filaments by light microscope. Filaments alone or in a 1:½ molar ratio actin:HMM were diluted to ≈10 nM

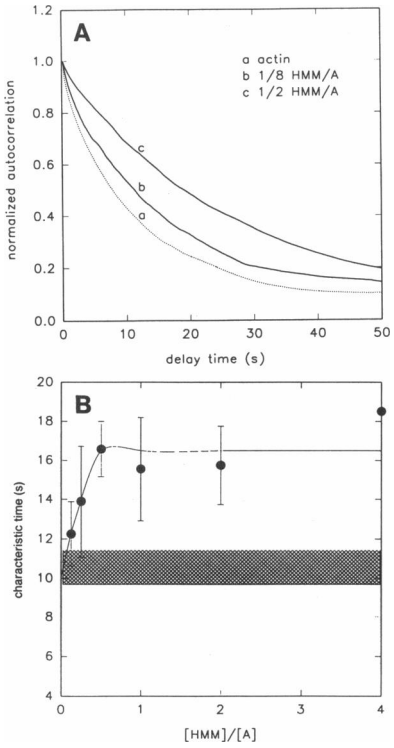

FIGURE 8 Normalized autocorrelation functions for 50 nM TRITC-phalloidin-F-actin in A-buffer in the presence of HMM. (*A*) line *a*-actin alone, line *b*-1:8 molar ratio HMM:actin, and line *c*-1:2 molar ratio HMM:actin (*B*) Characteristic times calculated from the double exponential fit of the autocorrelation functions for HMM:actin molar ratios from 1:8 to 4:1 (average and SEM of 4 measurements). The solid line is a plot of Eq. 3 in the interval $0 < MR < 0.5$. For $MR > 0.5$ the value was taken as constant. The dashed area represents the range of values measured for actin filaments in the absence of HMM.

and applied to a coverslip coated with nitrocellulose. The image of the filaments used in these experiments is shown in Fig. 9. Only filaments that adhered to the cover slip were observed. Histograms were calculated as described in Methods. Fig. 10 *A* shows the length distribution of 580 actin filaments (the same filaments which were used to obtain ACF shown in Fig. 6). The number average length of the filaments was defined as $L_n = (\Sigma N_i X_i)/(\Sigma N_i)$, where X_i is the length assigned to every filament whose length, L_i, was larger than or equal to $X_i - 0.25$ μm, and smaller than $X_i + 0.25$ μm (i.e., all filaments that differed in length by less then 0.5 μm were assigned the same length). The weight average length was defined as $L_w = (\Sigma N_i X_i^2)/(\Sigma N_i X_i)$. L_n and L_w were 2.37 and 4.41 μm, respectively. The ratio $\zeta = L_w/L_n$, which is a measure of the deviation of the distribution from the exponential ($\zeta = 2$ for exponential distribution) was 1.86. Fig. 10 *B* shows the length distribution of 429 actin filaments after irrigation with HMM (1 HMM:2 actins, the same filaments that were used to obtain the ACF shown in Fig. 8 *A*, curve *c*). L_n, L_w and ρ were now 2.48, 4.67, and 1.88 μm, respectively. According to a nonpaired *t* test, the means were not significantly different at 95% level of confidence. We conclude that addition of HMM does not change the length distribution of filaments.

To test the possibility that HMM increased the stiffness of actin filaments, we compared end-to-end length and contour lengths of bare actin (Fig. 11 *A*) and of acto-HMM complex (Fig. 11 *B*). The flexibility parameter λ was defined as $\langle R^2 \rangle = (2/\lambda^2)[\lambda L - 1 + \exp(-\lambda L)]$ (Takebayashi et al., 1977), where R is the end-to-end length of a filament and L is its contour length. $\lambda^{-1} = L_{corr}$ is the correlation length of the filament. Large L_{corr} indicates rigid filaments. λ was calculated from the best fit to data in Fig. 11. It is seen that correlation length is the same before and after incubation with HMM, indicating that the flexibility of filaments is the same when HMM is added.

At a constant temperature, fixed length distribution and constant flexibility of the diffusing species, τ_D depends only on the volume of the diffusing particles. Neither the length distribution nor flexibility were affected by the addition of HMM (Figs. 10 and 11) and assuming that the volume is proportional to the molecular mass and that $MR_{bound} \approx MR_{added}$, the best approximation for the increase in τ with MR in the interval $0 < MR < 1$ is

$$\tau_D = C \cdot (M_{actin} + MR \cdot M_{HMM})^{1/3} \qquad (3)$$

where C is a proportionality constant that includes temperature, average density of proteins, and the shape factor of the average actin filament, and M_{actin} and M_{HMM} are the molecular masses of actin filament and of HMM. The fact that τ_D depends on a third root of volume shows that the diffusion coefficient is inversely proportional to a linear dimension characteristic of a filament.

Acto-HMM-MgATP-γ-S

We wanted to see how the diffusion of acto-HMM was influenced by ATP-γ-S, an ATP analogue that traps heads in a weak binding configuration. 2 mM of ATP-γ-S was added to acto-HMM at $0.25 < MR < 2$. In each case, actin filaments moved as fast (but no faster) as bare actin filaments.

Acto-HMM-MgATP

When 2 mM MgATP was added to acto-HMM complex, the correlation time decreased (diffusion coefficient increased). At certain MR it decreased beyond τ of actin filaments alone. This is illustrated in Fig. 12 *A*, which shows the representative ACFs of actin alone (dotted line), acto-HMM complex in the presence of ATP when the ratio of HMM to actin was 1:8 (solid line *b*) and the complex in the presence of ATP at a MR of HMM to actin of 2:1 (solid line *c*). Data from all experiments is summarized in Fig. 12 *B*. Here the characteristic time of the acto-HMM complex in the presence of ATP is plotted versus the molar ratio HMM:actin. For comparison,

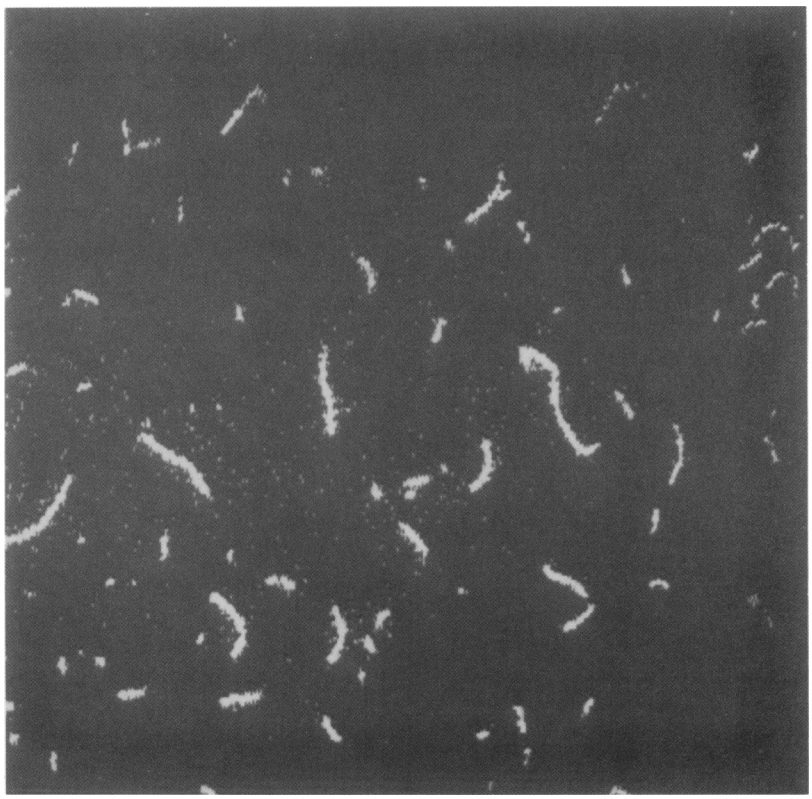

FIGURE 9 Image of 10 nM actin filaments labeled with TRITC-phalloidin and attached to a cover slip in A-buffer, recorded through a 100× objective.

the range of characteristic times of actin filaments alone is shown (mean ± SEM, shadowed area). The characteristic time decreased from the maximum of 11.76 s at the *MR* of HMM:actin = 4 to the minimum of 7.04 ± 0.34 at the ratio HMM:actin of 0.5.

There are four possible reasons why addition of ATP could decrease τ_D: (*a*) ATP could change the size distribution of acto-HMM so as to make the average length of filaments shorter; (*b*) ATP could increase the flexibility of acto-HMM (increase in the flexibility is associated with a decrease in τ_D, see Discussion); (*c*) hydrolysis of ATP could increase temperature of the sample; and (*d*) hydrolysis of ATP could impart extra velocity to actin. We show below that reasons 1–3 are not contributing to an observed decrease in τ_D. To examine the possibility (a), we directly observed filaments under a light microscope. Fig. 13 *A* shows the length distribution of actin filaments alone (the same as Fig. 10 *A*). Fig. 13 *B* is the distribution of 421 acto-HMM filaments in the presence of ATP (the same filaments that were used to obtain the ACF of Fig. 12 *A*, curve *c*). There was no significant change in average length or shape of distribution (as judged by ρ) in the two cases. To examine the possibility (b) we followed the same procedure as before, i.e., we compared end-to-end length and contour lengths of bare actin (Fig. 14 *A*) and of acto-HMM–ATP complex (Fig. 14 *B*). The flexibility parameter λ was defined as described above. λ was calculated from the best fit to data in Fig. 14. Correlation length was greater for acto-HMM–ATP complex than for bare actin, indicating that the flexibility of filaments decreased (and not increased) when ATP was added. This observation rules out the possibility that the observed decrease in τ_D is due to the increase in the flexibility. To examine possibility (c), we replaced HMM with apyrase at the concentrations liberating 1 and 10 P_i per head per second. The τ_D of a solution containing F-actin and apyrase (11.1 s) did not differ significantly from τ_D of a solution containing F-actin alone (9.1 s).

DISCUSSION

Method

Translational motion of acto-HMM complex is not an optimal indicator of binding of HMM to actin but FCS is one of a few tools capable of measuring motions of extremely dilute solutions. At very low acto-HMM concentrations, not enough light is scattered to attempt quasi-elastic light scattering (QELS) measurements. The concentration of F-actin used in the present experiments was 20 times lower than the lowest concentration used in QELS measurements (but still above critical concentration for phalloidin-actin, Yanagida et al., 1984). The

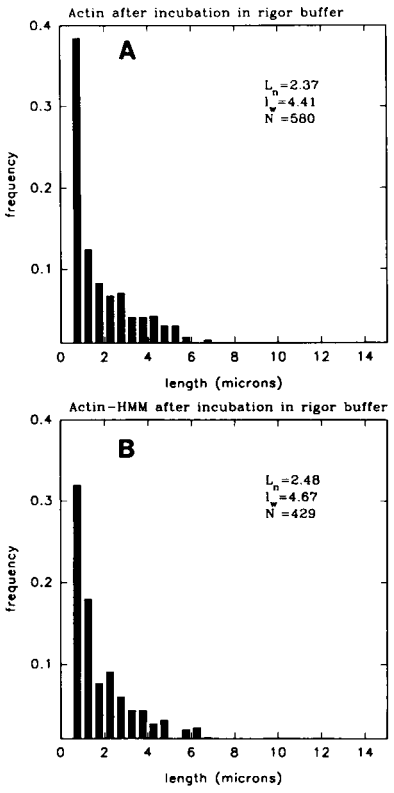

FIGURE 10 Length distribution of actin filaments labeled with TRITC-phalloidin, in A-buffer. (*A*) actin without HMM. (*B*) actin in the presence of 1/2:1 molar ratio:actin

hydrodynamic methods (Tanford, 1963) and even anisotropy decay (Highsmith et al., 1976) are too insensitive to measure motions of nM concentrations of proteins. Experiments of Fujime et al. (1984) indicate that motion of F-actin undergoes change as the solute is progressively diluted. It follows that the hydrodynamic measurements done at high actin concentrations cannot be extrapolated to low concentrations. The method is particularly suitable for measuring diffusion of F-actin labeled with phalloidin, because the quantum yield of phalloidin increases 10-fold when it binds to F-actin (Haugland et al., 1992).

Control experiments with spheres indicate that the method is reliable in measuring characteristic time. Earlier, we have applied the correlation method to measure the average velocity of actin filaments in two dimensions (in in vitro motility assay Borejdo and Burlacu, 1992*b*) and have achieved similar accuracy. Control experiments also show that, in spite of the fact that diffusion takes place in three dimensions, the two-dimensional analysis of FCS results correctly estimates the diffusion coefficient.

Actin filaments

Like in the case of spheres, the range within which all experimental ACFs of F-actin were contained was small. The characteristic time of all ACFs was 7.36 s $< \tau_D <$ 12.78 s. Two-dimensional analysis applied to actin results gives the diffusion coefficient $D_D = 0.9 \times 10^{-9} \pm 0.07 \times 10^{-9}$ cm^2 sec^{-1}. This is lower than the value measured by quasi-elastic light scattering by Fujime et al., 1972 (1.69×10^{-8} cm^2 sec^{-1}), Newman and Carlson, 1980 (1.24×10^{-8} cm^2 sec^{-1}) and Tirosh et al., 1990 (0.7×10^{-8} cm^2 sec^{-1}), but higher than measured by Schmidt et al., 1989 (8×10^{-11} cm^2 s^{-1}).

Acto-HMM

To test whether the observed increase in τ_D was caused by a decrease in the flexibility of the filaments, we compared correlation length of actin filaments, λ, before and after addition of HMM. HMM did not increase the average length of actin filaments (Fig. 10). λ of actin polymers was first measured by Fujime (1972) by QELS, and later by Takebayashi et al. (1977) directly from EM images of F-actin. The mean value of L_{corr} reported here before adding HMM, 7.9 μm (Fig. 11 *A*) is comparable to the correlation length estimated from the EM. L_{corr} increased to 8.3 μm after adding HMM (Fig. 11 *B*), but the difference was not statistically significant. Bare actin filament has high bending modes and HMM eliminates these modes, as shown by Thomas et al. (1979). How-

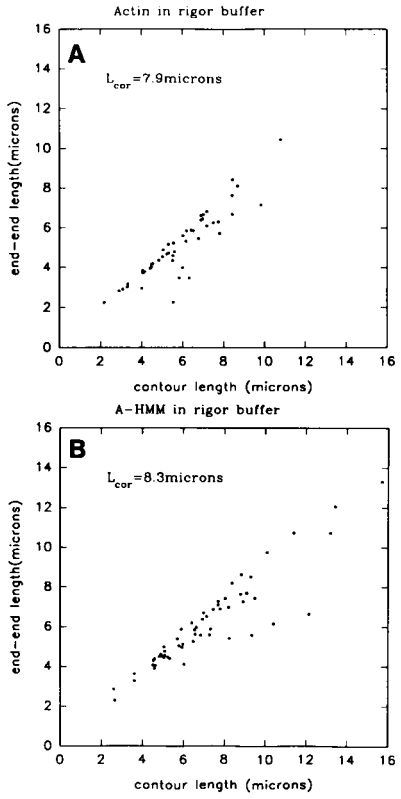

FIGURE 11 End-to-end versus contour length of (*A*) actin filaments and (*B*) actin filaments in the presence of 1:1 molar ratio HMM:actin, both in A-buffer.

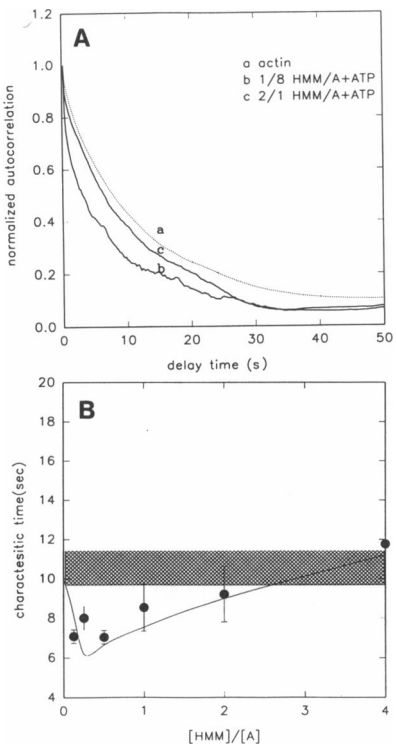

FIGURE 12 (*A*) Normalized autocorrelation functions of 50 nM actin filaments suspended in A-buffer containing 2 mM MgATP at following molar ratios of HMM:actin: (*a*) 0, (*b*) 1/8, and (*c*) 2/1. (*B*) Characteristic times of the autocorrelation functions of actin filaments in the presence of HMM and MgATP versus HMM:actin molar ratio. The solid line is a plot of Eq. 4, with $\phi = 0.1$, H = 250 sec. The dashed area represents the domain of values measured for actin in the absence of HMM.

ever, stiffness as defined here, was the same when measured in an optical microscope and in EM (Burlacu et al., 1992). We conclude that the increase in τ_D (slower diffusion) resulted only from an increase in the volume of the complex. The increase in τ_D reached maximum when the *MR* of HMM:actin was 0.5:1 (ratio of myosin heads:actin = 1). At this point, the molecular mass of the filament increased by over 400% but τ_D increased by less than 200%.

Large variability in τ at low *MR* (see Fig. 8 *B*) is consistent with the observation of Fujime and Ishiwata (1971) and Oosawa et al. (1973), who titrated F-actin with HMM and measured broadening of spectrum of quasi-elastically scattered light. They interpreted their results to suggest that at low *MR* HMM increased the flexibility of actin filaments. On the other hand, our result, showing that at larger *MR* HMM decreased the diffusion coefficient, contrasts with the results of these authors who suggested that HMM caused no change in the diffusion coefficient. It is possible that the difference is associated with the use of high concentrations of F-actin in QELS experiments, giving an opportunity for bifunctional HMM to aggregate (cross-link) filaments. In fact, at high concentrations of F-actin we sometimes observed such aggregation under the microscope. Our data are inconsistent with the results of Yanagida and Oosawa (1978), who reported increase in flexibility of thin filaments in muscle at large molar ratios of HMM:actin.

Acto-HMM-MgATP-γ-S

We estimate that, under our experimental conditions, there are on the average ten molecules of HMM bound to each filament in the presence of ATP-γ-S. Our results suggest that these ten molecules do not retard diffusion of actin filaments. This is not surprising, considering that in rigor, even at a molar ratio of HMM to actin of 1:16 (i.e., 62 strongly bound cross-bridges per filament), there was only a slight retardation of diffusion. Our finding is consistent with the observation of Uyeda et al. (1991) that in the in vitro motility assay, upon addition of MgATP-γ-S, the actin filaments escaped from HMM immobilized on a glass surface. The fact that muscle fibers show significant stiffness in the presence of MgATP-γ-S (Dantzig et al., 1988) is most likely due to large effective protein concentration.

Acto-HMM-MgATP

The unexpected result was that during hydrolysis of ATP the diffusion of actin filaments in the presence of HMM was accelerated. The difference in τ_D values between ac-

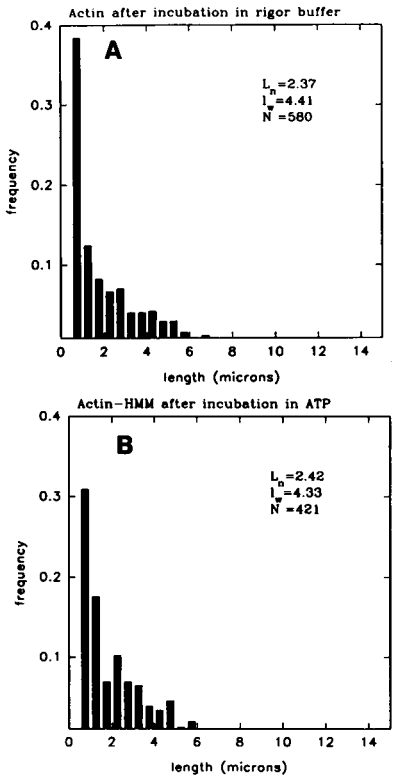

FIGURE 13 Length distribution of actin filaments labeled with TRITC-phalloidin, in buffer A. (*A*) actin. (*B*) actin with 1:1 molar ratio HMM:actin and 2 mM MgATP.

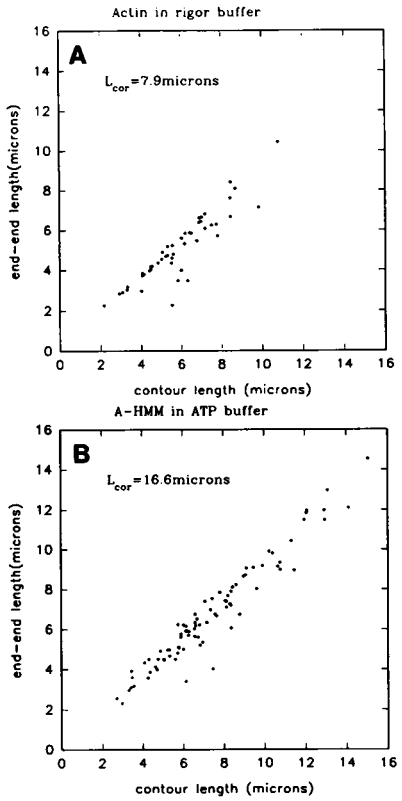

FIGURE 14 End-to-end versus contour length of (*A*) actin filaments in A buffer, (*B*) actin filaments in the presence of 1:1 molar ratio HMM:actin and 2 mM MgATP.

tin alone and acto-HMM complex in the presence of ATP was statistically significant at low *MR* of HMM:actin (in nonpaired *t* test the values for significance of the difference at 5% level were: $t = 2.94$, $P = 1.64 \times 10^{-2}$ at HMM:actin = 0.125; $t = 2.56$, $P = 3.35 \times 10^{-2}$ at HMM:actin = 0.25; and $t = 2.58$, $P = 3.27 \times 10^{-2}$ at HMM:actin = 0.5). At higher *MR* the difference was not statistically significant ($t = 1.36$, $P = 2.11 \times 10^{-1}$ at HMM:actin = 1.0; and $t = 8.88 \times 10^{-1}$, $P = 4.00 \times 10^{-1}$ at HMM:actin = 2.0). The decrease seen at low *MR* was not due to a decrease in the average length of actin filament (Fig. 13) or to an increase in their flexibility (Fig. 14). In fact, the observation of filaments under microscope showed that the addition of ATP caused the filaments to become less flexible, as indicated by a decrease in λ (Fig. 14 *B*). Oosawa et al. (1973), on the other hand, measured the width of the spectrum of quasi-elastically scattered light during hydrolysis. From the observation that the width became smaller during ATPase they concluded that the flexibility of filaments increased. The present results are consistent with the observation of Yanagida et al. (1984), who reported that in the presence of HMM and ATP actin filaments executed rapid motions. We did not see filaments being broken into short fragments, but HMM concentration in our experiments was at least 1,000-fold lower.

Our results indicate that ATP caused a decrease in the flexibility of the filaments (Fig. 14). If this were the only effect of ATP, the diffusion coefficient would decrease (Wegener, 1982; Janmey, 1990). Instead, the diffusion coefficient increased, suggesting that the energy of hydrolysis of ATP resulting from the interaction of actin and HMM was imparted to the diffusing species (see below). The decrease in τ_D was not due to a rise in temperature: firstly the decrease was not seen at high *MR*, where amount of energy liberated by hydrolysis of ATP was higher, and secondly, control experiments with apyrase showed that hydrolysis alone had no effect on diffusion.

How is the diffusion of acto-HMM–ATP complex accelerated in comparison with the diffusion of bare actin during hydrolysis of ATP? Following Oplatka et al. (1974), we propose that some of the energy of hydrolysis of ATP resulting from the interaction of actin and HMM is imparted to the diffusing species. Thus HMM and solvent molecules receive equal amount of momentum (actin filaments are not directly involved in splitting because hydrolysis occurs while heads are dissociated from actin). We estimate that on the average, in the presence of ATP, one molecule of HMM is at any time bound to an actin filament. This results in splitting of about 40 molecules of ATP/s/filament. The energy liberated by this splitting is several orders of magnitude larger than the kinetic energy of a filament. Part of this energy is carried away by products of hydrolysis (or other small molecule, i.e., water). Part may be transferred to actin by recoiling HMM. Oplatka et al. (1974) suggested that most of the energy is carried away by water, in a direction defined by a polarity of a filament. Solvent is thus compelled to stream and carry actin with it. Regardless of the exact mechanism by which the energy is imparted to filaments, the macroscopic effect is demonstrated as faster translation of filaments.

The present data, and the results of Tirosh et al. (1990), who reported the broadening of spectrum of quasi-elastically scattered light from acto-HMM when the hydrolysis occurred, support the above interpretation.

In spite of the fact that motion of F-actin was accelerated during activation of ATPase activity by HMM, we did not observe any change in the diffusion of HMM upon interaction with actin in the presence of ATP (Borejdo, 1979; Borejdo and Burlacu, 1992*a*). This is most likely due to the low Reynolds number of a solvent, i.e., the fact that the motion of HMM decays shortly after leaving the vicinity of a filament. Acceleration of filament motion, however, occurs mainly along its long axis, where hydrodynamic resistance is the lowest.

Fraction of strongly and weakly bound heads during ATPase

We can now estimate a fraction of heads that slow down diffusion during hydrolysis. In our experiments, like in those reported by Tirosh et al. (1990), the enhancement

of diffusion disappeared at molar ratios higher than one. It suggests that the enhancement is a combination of the two effects: a rigor-like (strong) binding, which slows down the diffusion, and the acceleration due to the explosive splitting of ATP. The rigor binding slows down the diffusion according to Eq. 3, except that now only a fraction ϕ of HMM is strongly bound to F-actin at any time (we assume that this fraction is the same at each MR). Decrease in τ_D is assumed to be proportional to the number of interacting HMM molecules $\phi \cdot MR$. H is a constant that describes a decrease in characteristic time of actin filaments resulting from the interaction with 1 HMM in the presence of ATP. In the presence of ATP we thus get:

$$\tau_D = C \cdot (M_{actin} + \phi \cdot MR \cdot M_{HMM})^{1/3} - \phi \cdot MR \cdot H. \quad (4)$$

There are two parameters in Eq. 4—ϕ and H; nevertheless the data of Fig. 12 B can be fitted to Eq. 4 because ϕ and H have separate effects on the fit. Changing ϕ (at constant H) changes only the slope of the fit (without affecting the intercept), and changing H (for constant ϕ) shifts the intercept of the fit (without affecting the slope). The best fit was obtained with $\phi = 0.06 \pm 0.02$ and $H = 250 \pm 25$ s.

We thank Prof. W. W. Webb, Dr. I. Brust-Maschel and Prof. A. Oplatka for valuable comments.

This work was supported by a grant from the National Institutes of Health (AR-40095-01).

Received for publication 5 May 1992 and in final form 3 August 1992.

REFERENCES

Borejdo, J., and M. F. Morales. 1977. Fluctuations in tension during contraction of single muscle fibers. *Biophys. J.* 20:315–334.

Borejdo, J. 1979. Motion of myosin fragments during actin activated ATPase. Fluorescence correlation spectroscopy study. *Biopolymers.* 18:2807–2820.

Borejdo, J., and S. Burlacu. 1992*a*. Diffusion of heavy meromyosin in the presence of F-actin and ATP. *J. Muscle Res. Cell Motil.* 13:106–116.

Borejdo, J., and S. Burlacu. 1992*b*. Velocity of movement of actin filaments in in vitro motility assay measured by fluorescence correlation spectroscopy. *Biophys. J.* 61:1267–1280.

Burlacu, S., P. A. Janmey, and J. Borejdo. 1992. Distribution of actin filament lengths measured by fluorescence microscopy. *Am. J. Physiol. (Cell Physiol.)* 262:C569–C577.

Dantzig, J. A., J. W. Walker, D. R. Trentham, and Y. E. Goldman. 1988. Relaxation of muscle fibers with adenosine 5′-[Gamma-thio]-triphosphate (ATP[γ-S]) and by laser photolysis of caged ATP[Gamma-S]: Evidence for Ca^{2+}-dependent affinity of rapidly detaching zero-force cross bridges. *Proc. Natl. Acad. Sci. USA.* 85:6176–6720.

Elson, E. L., and D. Magde. 1974. Fluorescence correlation spectroscopy. I. Conceptual basis and theory. *Biopolymers.* 13:1–28.

Elson, E. L., and W. W. Webb. 1975. Concentration correlation spectroscopy. *Annu. Rev. Biophys. Bioeng.* 4:311–334.

Elson, E. L., and H. Qian. 1989. Interpretation of fluorescence correlation spectroscopy and photobleaching recovery in terms of molecular interactions. *Methods Cell Biol.* 30:307–332.

Englander, S. W., D. B. Calhoun, and J. J. Englander. 1987. Biochemistry without oxygen. *Anal. Biochem.* 161:300–306.

Fraser, A. B., E. Eisenberg, W. W. Kielley, and F. D. Carlson. 1975. The interaction of heavy meromyosin and subfragment-1 with actin. Physical measurements in the presence and absence of adenosine triphosphate. *Biochemistry.* 14:2207–2214.

Fujime, S., and S. Ishiwata. 1971. Dynamic study of F-actin by quasi-elastic scattering of laser light. *J. Mol. Biol.* 62:251–265.

Fujime, S. 1972. Quasi-Elastic Scattering of Laser Light—A New Tool for the Dynamic Study of Biological Macromolecules. *Adv. Biophys.* 3:1–39.

Fujime, S., S. Ishiwata, and T. Maeda. 1972. F-actin-heavy meromyosin complex studied by optical homodyne and heterodyne methods. *Biochem. Biophys. Acta.* 283:351–363.

Goldman, Y. E., M. G. Hibberd, and D. R. Trentham. 1984. Initiation of active contraction by photogeneration of adenosine-5′-triphosphate in rabbit psoas muscle fibers. *J. Physiol.* 354:605–624.

Harada, Y., K. Sakudara, T. Aoki, D. D. Thomas, and T. Yanagida. 1990. Mechanochemical coupling in actomyosin energy transduction studied by *in vitro* movement assay. *J. Mol. Biol.* 216:49–68.

Haugland, R. P., Z. Huang, R. P. Haugland, V. Paragas, W. You, and S. Wells. 1992. Interaction of phalloidin with actin. *Proc. Conf. Muscle as a Machine: Energy Transduction in the Contractile System.* Bethesda, MD. April 13–15, 1992. (Abstr.)

Highsmith, S., R. A. Mendelson, and M. F. Morales. 1976. Affinity of myosin S1 for F-actin, measured by time resolved fluorescence anisotropy. *Proc. Natl. Acad. Sci. USA.* 73:133–137.

Houseal, T. W., C. Bustamante, R. Stump, and M. F. Maestre. 1989. Real time imaging of single DNA molecule with fluorescence microscope. *Biophys. J.* 56:507–516.

Huxley, H. E. 1969. The mechanism of muscular contraction. *Science (Wash. DC).* 164:1356–1366.

Janmey, P. A., S. Hvidt, G. F. Oster, J. Lamb, T. P. Stossel, and J. H. Hartwig. 1990. Effect of ATP on actin filament stiffness. *Nature* (Lond.). 347:95–99.

Koppel, D. E. 1974. Statistical accuracy in fluorescence correlation spectroscopy. *Phys. Rev. A.* 10:1938–1945.

Kron, S. J., and J. A. Spudich. 1986. Fluorescent actin filaments move on myosin fixed to a glass surface. *Proc. Natl. Acad. Sci. USA.* 83:6272–6276.

Lymn, R. W., and E. W. Taylor. 1971. Mechanism of adenosine triphosphate hydrolysis by actomyosin. *Biochemistry.* 10:4617–4624.

Magde, D., E. L. Elson, and W. W. Webb. 1974. Fluorescence correlation spectroscopy. II. An experimental realization. *Biopolymers.* 13:29–61.

Newman, J., and F. D. Carlson. 1980. Dynamic light scattering evidence for the flexibility of native muscle thin filaments. *Biophys. J.* 29:37–47.

Oosawa, F., S. Fujime, S. Isiwata, and K. Mihashi. 1973. Dynamic property of F-actin and thin filament. *Cold Spring Harbor Lab.* 37:277–285.

Oplatka, A., H. Gadasi, R. Tirosh, Y. Lamed, A. Muhlrad, and N. Liron. 1974. Demonstration of mechanochemical coupling in systems containing actin, ATP and non-aggregating active myosin derivatives. *J. Mechanochem. Cell Motil.* 2:295–306.

Podolsky, R. J. 1980. The rate-limiting step in muscle contraction. *Basic Res. Cardiol.* 75:34–39.

Qian, H., and E. L. Elson. 1990. Characterization of confocal laser based microscope by digital image analysis—an optical sectioning microscopy approach. *In* Optical Microscopy for Biology. B. Herman and K. Jacobson, editors. Alan R. Liss, New York. 119–130.

Qian, H., and E. L. Elson. 1991. Analysis of confocal laser-microscope

optics for 3-D fluorescence correlation spectroscopy. *Appl. Optics.* 30:1185–1195.

Rabiner, L., and B. Gold. 1975. *In* Theory and Application of Digital Signal Processing, Prentice-Hall, Englewood Cliffs, NJ. 367.

Schmidt, C. F., M. Barmann, C. Isenberg, and E. Sackmann. 1989. Chain dynamics, mesh size, and diffusive transport in networks of polymerized actin. A quasielastic light scattering and microfluorescence study. *Macromolecules.* 22:3638–3649.

Spudich, J., and S. Watt. 1971. The regulation of rabbit skeletal muscle contraction. I. Biochemical studies of the interaction of the tropomyosin-troponin complex with actin and the proteolytic fragments of myosin. *J. Biol. Chem.* 246:4866–4871.

Takebayashi, T., Y. Morita, and F. Oosawa. 1977. Electronmicroscopic investigation of the flexibility of F-actin. *Biochem. Biophys. Acta.* 492:357–363.

Tanford, C. 1963. *In* Physical Chemistry of Macromolecules, John Wiley and Sons, New York. 362.

Tirosh, R., W. Z. Low, and A. Oplatka. 1990. Translational motion of actin filaments in the presence of heavy meromyosin and MgATP as measured by Doppler broadening of laser light scattering. *Biochem. Biophys. Acta.* 1037:274–280.

Thomas, D. D., J. C. Seidel, and J. Gergely. 1979. Rotational dynamics of spin-labeled F-actin in the submillisecond time range. *J. Mol. Biol.* 132:257–273.

Uyeda, T. Q. P., H. M. Warrick, S. J. Kron, and J. A. Spudich. 1991. Quantitized velocities at low myosin densities in an in vitro motility assay. *Nature (Lond.).* 352:307–311.

Yanagida, T., and F. Oosawa. 1978. Polarized fluorescence from ϵ-ADP incorporated into F-actin in a myosin free single fiber: conformation of F-actin and changes induced in it by heavy meromyosin. *J. Mol. Biol.* 126:507–524.

Yanagida, T., M. Nakase, K. Nishiyama, and F. Oosawa. 1984. Direct observation of motion of single F-actin filaments in the presence of myosin. *Nature (Lond.).* 307:58–60.

Yanagida, T., T. Arata, and F. Oosawa. 1985. Sliding distance of actin filament induced by myosin cross-bridge during one ATP hydrolysis cycle. *Nature (Lond.).* 316:366–369.

Wegener, W. A. 1982. Bead models of segmentally flexible macromolecules. *J. Chem. Phys.* 76:6425–6430.

Weeds, A. G., and B. Pope. 1977. Studies on the chymotryptic digestion of myosin. Effects of divalent cations on proteolytic susceptibility. *J. Mol. Biol.* 111:129–157.